Control of Magnetic Anisotropies in Sputter-Deposited Yttrium Iron Garnet (YIG)

Camille Bean, Vincent Humbert, Junseok Oh, Joseph Sklenar, Nadya Mason
Harvard University and Department of Physics, University of Illinois at Urbana-Champaign

ABSTRACT

Yttrium iron garnet, or YIG, is a ferrimagnetic insulator with a low Gilbert damping constant, making it a favorable candidate for spintronics and magnetization dynamics studies, especially when it has perpendicular magnetic anisotropy (PMA). To fabricate YIG with PMA, strain can be induced in a thin film of YIG by sputtering onto $Gd_3(Sc_2Ga_3)O_{12}$ (GSGG). We report our effort to optimize the epitaxial growth of sputter-deposited YIG films. YIG films grown on $Gd_3Ga_5O_{12}$ (GGG) substrates were characterized by X-ray diffraction (XRD) for crystal structure and a Quantum Design Magnetic Property Measurement System (MPMS) for magnetization. A YIG film of approximately 57% of bulk magnetization was grown on GGG, with signs of crystallization in the (111) orientation.

I. Background and Introduction

$Y_3Fe_5O_{12}$, or yttrium iron garnet (YIG), is a ferrimagnetic insulator. Because of its low Gilbert damping parameter, it's useful in studies of magnetization and spintronics applications. The Gilbert damping parameter describes the stability of excitations; a low Gilbert damping parameter means that excitations will slowly relax to the equilibrium, which is useful for magnetization studies. The insulating properties of YIG also make it a good candidate for transport studies in magnetically proximitized heterostructures.

Due to its ferrimagnetism, YIG has magnetic anisotropy, which is the directionality of its magnetic moment. Anisotropy may be in the plane of the sample, perpendicular to the plane of the sample, or some other direction. YIG films are generally grown by sputtering onto $Gd_3Ga_5O_{12}$ (GGG), and these YIG/GGG growths favor in-plane anisotropy. However, varying the gas flow, sputtering power, and chamber pressure across growths can influence the anisotropy to have other configurations. The film structure of the sample also influences the magnetic response, with stronger magnetization in the monocrystalline form.

The perpendicular magnetic anisotropy (PMA) is favorable for spintronics applications, so being able to reliably acquire the PMA is an important part of studying YIG. Being able to produce the PMA reliably could even open possibilities for device fabrication within the work of the Mason lab. For example, topological inductors or switches might be built on top of YIG films.

In addition to using the sputtering parameters to influence the anisotropy, varying the substrate can have a strong effect. Gang Li et al. achieved YIG with PMA by sputtering on substrates that have lattice constants that exceed YIG by a ratio of 0.76% to 1.58%. These substrates included $Y_3(Sc_2Ga_3)O_{12}$ (YSGG), $(Gd_{0.63}Y_{2.37})(Sc_2Ga_3)O_{12}$ (GYSGG), and $Gd_3(Sc_2Ga_3)O_{12}$ (GSGG).[1]

By varying the substrate, the strain between the YIG film and substrate was changed. In the work by Gang Li et al., YIG with PMA was grown on GSGG to 10nm.

However, for 15nm and 30nm samples, the strain had already been reduced to such an extent that in-plane anisotropy persisted.[1]

The goal of this project is to optimize the epitaxial growth of YIG films grown in an AJA sputtering chamber, and to control the anisotropy of these films to be in-plane or out-of-plane. The parameters of gas flow, sputtering power, and chamber pressure were varied in the pursuit of this result. The crystalline structures of growths on GGG were assessed by X-ray diffraction (XRD) and the magnetization was assessed using a Quantum Design Magnetic Property Measurement System (MPMS).

II. Method

YIG samples were grown in an AJA sputtering system. Sputtering was done off-axis, with the sample mounted 2 inches above and 2 inches away from the YIG target. Two strike layers with an open shutter were used to achieve plasma. During growth, the stage was rotated for even deposition. Samples were then annealed to create monocrystalline structure. After annealing, samples were analyzed for crystalline structure and magnetic anisotropy. The complete record of sample parameters can be found in figure 1.

Figure 1:

Sample #	1	2	3	4
Substrate	GGG	GGG	GGG	GGG
Growth Parameters	30 sccm Ar, 3mT, 100W	30 sccm Ar, 3mT, 100W	30 sccm Ar, 3mT, 100W	16 sccm Ar, 10mT, 75W
Thickness (nm)	26	40	26	63
Anneal	800° C 3hr in air, 900° C 3 hr in air	900° C 3 hr in air	800° C 2hr in oxygen (120° C/hr heating, 180° C/hr cooling)	800° C 3hr in air (120° C/hr heating, 180° C/hr cooling)

For samples 1, 2, and 3, the sputtering occurred at 30 sccm argon flow, 3mT chamber pressure, and 100W sputtering power. These parameters were taken from the YIG growth calibration done on the sputtering system by staff at the Illinois Materials Research Laboratory. After failing to see results improve, even with a thicker film, the parameters were changed to 16 sccm flow, 10mT chamber pressure, and 75W sputtering power for sample 4. These parameters were taken from a paper by Shaozhen Li et al., where YIG was sputtered on GGG. [2]

For samples 1 and 2, annealing was done without attention to the ramping rates for heating or cooling. Because of the importance of the anneal to surface structure, this parameter was later controlled for. For samples 3 and 4, heating was done at a rate of 120° C while cooling was done at a rate of 180° C. Sample 3 was annealed in oxygen, while sample 4 was annealed in open air.

Sample crystalline structure was determined by X-ray diffraction (XRD), using a Philips X'Pert system. In XRD, an x-ray

source (held at some angle ω from the sample) sends X-rays into a sample, and the reflected rays are measured by a detector (held at some angle θ from the sample). The detected X-rays are used to determine the crystal structures present in the sample as well as their orientations. Measurements were taken using a 2θ-ω scan type, in which both the detector and source are mobile during the scan. Measurements were done in two ranges: a broad scan (from 10-100° 2θ) and a close scan around the YIG and GGG (444) peaks (from 49.5-53.5° 2θ).

Magnetic anisotropies were determined using a Quantum Design Magnetic Property Measurement System (MPMS). The MPMS introduces magnetic fields to a sample and measures the resulting moment with a superconducting quantum interference device (SQUID), which is extremely sensitive to magnetic fields. The GGG samples were mounted to a quartz rod using GE varnish, and the magnetic field was applied parallel to the plane of the sample surface.

For every change in the growth parameters, the thickness of the deposition was tested. This was done by simultaneously sputtering onto an SiO_2 chip that had been patterned by photolithography before sputtering. The pattern step height was measured by atomic force microscopy afterward.

III. Results

The expected peak values for YIG (111) and GGG (111), taken from database values for the bulk, are within 0.02° 2θ of each other for each respective peak. [3] Because of this, at the resolution of the 10-100 scans, they are indistinguishable. For XRD on GGG (111) samples, peaks are visible at the (222) and (444), whether YIG is present or not. The (666) peak only appeared on sample 1 (see figure 2). All labels in figure 2 refer to the sample numbers given in figure 1.

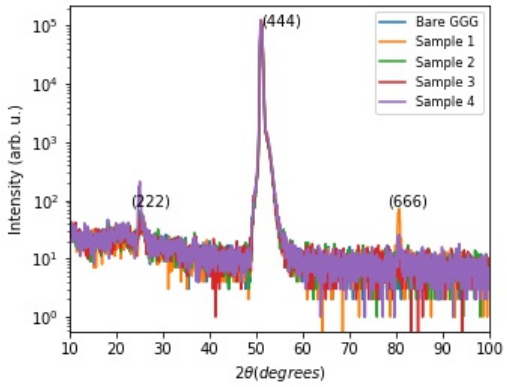

Figure 2a: Various YIG/GGG sample peaks are visible at the (222), (444), and (666).

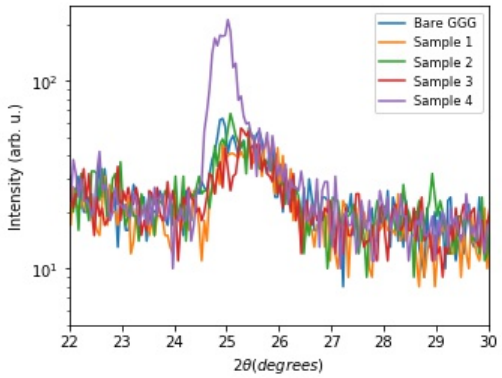

Figure 2b: Around (222), all sample peaks are similar, including bare GGG, except for 444, which has a much stronger response on the left side.

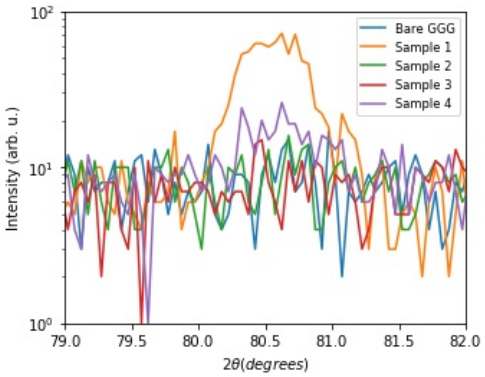

Figure 2c: Only the 26nm YIG/GGG sample shows the 666 peak

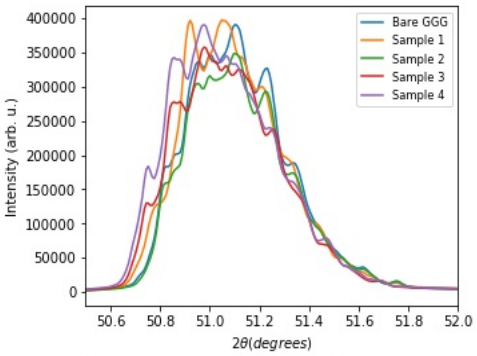

Figure 2d: The shapes for the bare GGG and sample 2 are similar to each other, and the shapes for samples 3 and 4 are simliar to each other, with some variation in intensity within each pair.

In the (222) peak, all responses are similar except for sample 4, which has a stronger response to the left side of the peak.

The scans around the (444) peak show similar shape between sample 2 and bare GGG. They both have a feature to the right of the main peak, at around 51.3° 2θ. The intensity of the bare GGG peaks are stronger, but the units are arbitrary, so they cannot be compared as a manner of absolute measure. The shapes for samples 3 and 4 are also similar to each other, with a feature to the left of the main peak, at around 50.9° 2θ. Sample 1 also has a feature towards the left, at around 50.8° 2θ.

For the MPMS measurements, we expect that because the substrate is 0.5 mm thick and the growth is tens of nanometers thick, that the strongest response will be from the paramagnetic signal of GGG substrate, which is linear with field. To counter this effect, MPMS data from the GGG samples were fit to a linear regression, for some linear portion of the data where YIG magnetization is considered to be fully saturated. Fitting over the entire set would cause any hysteresis features to alter the linear fit. Figure 3a shows an example of the linear fit method.

Then, the residual of the fit was taken to be the moment of the YIG film. The simple relation $magnetization = \frac{moment}{volume}$ was used to determine the magnetization and saturation magnetization M_S. The magnetization graphs are figures 3b-d. Sample 1 shows a saturation magnetization of ~40 emu/cm^3, sample 2 shows a saturation magnetization of ~60 emu/cm^3, sample 3 showed no YIG magnetization, and sample 4 showed ~80 emu/cm^3 (see figure 3).

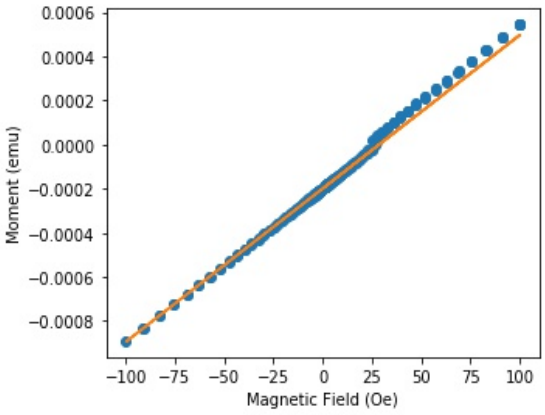

Figure 3a: The data from sample 1, fit from -100 to 0 Oe. The raw data is shown as blue dots, and the linear fit is shown in orange.

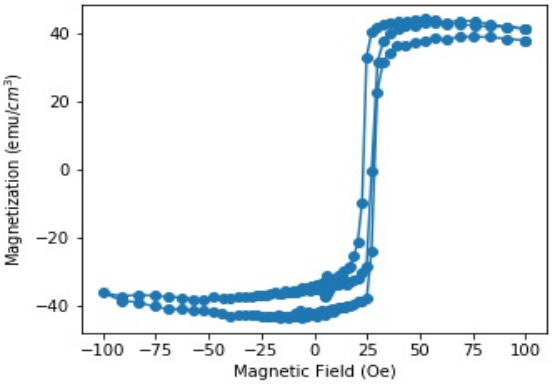

Figure 3b: The residual magnetization from the linear regression from figure 3a.

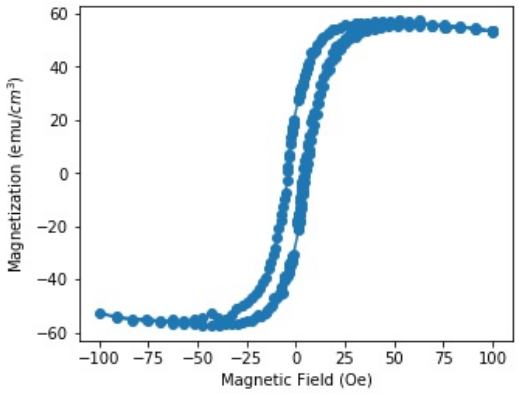

Figure 3c: Residual magnetization from a regression on sample 2, fit from -100 to -25 Oe.

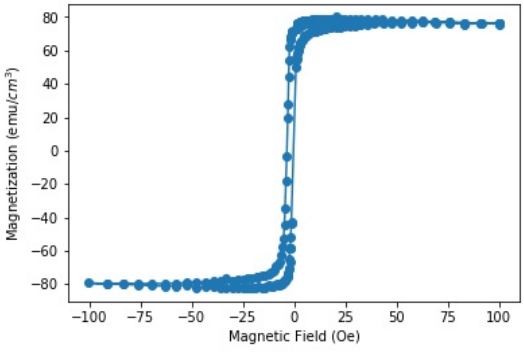

Figure 3d: Residual magnetization from a regression on sample 4, fit from -100 to -25 Oe.

VI. Discussion

According to the values taken from International Centre for Diffraction Data, the 2θ values for the bulk forms of YIG and GGG are, respectively, 24.9257° and 24.9216° at (222), 51.1399° and 51.1331° at (444), and 80.6946° and 80.6789° at (666).[3] Given that the maximal difference between the peaks is 0.0157° at (666), it would seem that detecting the difference between the peaks would be extremely difficult. However, the configuration of the YIG/GGG samples does not represent that of two bulk materials.

Because of the strain between the substrate and film layer, the YIG (444) peak is shifted to a significantly lower 2θ, making the difference between the peaks more easily detectable. In work done on similar YIG/GGG samples, the YIG (444) peak tends to appear at around 50.8°. [2 4 5] A visible feature in this position, differing from the GGG (444) peak found near 51.1°, can be taken as an indication of YIG (111).

The XRD scans of sample 2 and bare GGG samples around 444 looked very similar (see figure 2a). It's likely that monocrystalline YIG was not achieved in sample 2, so no prevailing YIG (444) peak could be found to compete with the effects of the GGG (444) peak. At first, it was considered that maybe growing a thick layer had caused a reduction of strain that caused the (444) peaks to be closer to their bulk positions. However, sample 4, which is even thicker, does not take on the same shape.

In samples 3 and 4, there is a shoulder around 50.8° that does not appear in sample 2 or the bare GGG. This is the position where YIG (444) is found in the literature, and this points towards the presence of YIG (111) in samples 3 and 4.

In sample 1, there is a similar feature at around 50.9°. This could be evidence of YIG (111), but the overall shape of the peak is dissimilar from the other scans in general, so it's harder to interpret this result.

The (222) peaks look similar in all scans except for sample 4. Perhaps, although the (222) peak is present for GGG, the left side of the peak gains intensity with the presence of YIG (111). Otherwise, intensity disparities may depend on the positioning of the sample in the XRD system, in such a generally weak response.

The (666) peak appears only for sample 1. This response is not clear, but once again, it may be due to positioning of the sample, given such a generally weak response at this peak.

Overall, XRD showed convincing evidence for the presence of YIG (111) in samples 3 and 4, with weaker evidence of its

presence in sample 1. There was no evidence of crystallized YIG in sample 2, and there was no apparent correlation of XRD response with sample thickness.

In all samples, the values for saturation magnetization were lower than expected, although hysteresis loops were clear. Other papers with YIG/GGG samples found the value to be around 130-140 emu/cm^3. [2 5] Sample 1 showed 40 emu/cm^3, sample 2 showed 60 emu/cm^3, and sample 4 showed 80 emu/cm^3. There is some correlation between thicker samples and higher saturation magnetization, but given the limited number of samples and the variation in their procedures, this relationship is unclear.

The possible causes of the disparity between literature and experimental values for saturation magnetization are the sputtering parameters and the anneal program.

For samples 1, 2, and 3, sputtering was done with parameters taken directly from the YIG calibration growths done by staff at the Illinois Materials Research laboratory. For these settings, saturation magnetization was less than half of the expected values. After changing to the parameters taken from a paper by Shaozhen Li et al., the magnetization improved greatly, and the hysteresis loop was visibly narrower. [2] Perhaps because these parameters were chosen specifically for YIG/GGG growths, they are better suited to yield the magnetization that we hope to achieve.

For samples 1 and 2, annealing was done using the automatic ramping rates of the tube furnace. After beginning to control the heating and cooling rate, samples 3 and 4 showed evidence of crystallized YIG (111). However, Sample 3 showed no YIG magnetization, which was unexpected. It may be that 2 hours at 800° C was insufficient to anneal completely, since all previous samples had shown some magnetization, even if it wasn't to the expected degree. Sample 4, which was annealed at 800° C for 3 hours, showed better crystallization and magnetization than any previous samples. This is likely attributable partially to the new sputter settings and partially to the controlled anneal.

V. Conclusions

YIG was sputtered onto GGG to grow films with in-plane anisotropy. MPMS scans showed that YIG films had saturation magnetization of up to 80 emu/cm^3, which is below the values found in the literature. XRD scans showed some evidence of crystallization for some samples. While these results are promising, there is plenty of work that could be done to expand on the epitaxial sputtering of YIG films.

First, some improvements could be made in the magnetization. Magnetization in GGG improved over the course of the trials. However, it never reached the expectations based on data from similar samples in literature. Changing the growth parameters between samples 3 and 4 made great improvements, and perhaps continuing to adjust the chamber pressure, sputter power, and argon flow could improve the magnetization.

The magnetization might also be improved by adjusting the annealing procedure. Ramping to and from the annealing temperature can affect the structure of the sample, and this can be controlled in the hopes of achieving different results. Other ramping rates could be used. For example, one could cool the samples to room temperature more rapidly, in an effort to preserve the strain between substrate and film.

Also, the PMA has not been attempted yet in this project. GGG samples have been used, and we have seen in-plane anisotropy,

but we only expect to see PMA for samples grown on GSGG. With improvements in magnetization, the sample focus could shift towards attempting growths with PMA.

VI. Acknowledgments

This material is based upon work supported by the National Science Foundation under Grant PHY-1659598. Any opinions, findings, and conclusions or recommendations expressed in this material are those of the author(s) and do not necessarily reflect the views of the National Science Foundation.

The author acknowledges the use of facilities and instrumentation supported by the NSF through the University of Illinois Materials Research Science and Engineering Center DMR-1720633.

The author would like to thank the Mason Group for support. Sample fabrication and analysis were performed in the Frederick Seitz Materials Research Lab at the University of Illinois.

VII. References

1. Gang Li, He Bai, Jian Su et al, "Tunable perpendicular magnetic anisotropy in epitaxial $Y_3Fe_5O_{12}$ films," *APL Materials* **7,** 041104 (2019).
2. Shaozhen Li, Wei Zhang, Junjia Dong et al, "Epitaxial patterning of nanometer-thick $Y_3Fe_5O_{12}$ films with low magnetic damping," *Nanoscale* **8**, 388-394 (2016).
3. ICDD (2018). PDF-4+ 2019 (Database), edited by Dr. Soorya Kabekkodu, International Centre for Diffraction Data, Newtown Square, PA, USA
4. Houchen Chang et al, "Nanometer-Thick Yttrium Iron Garnet Films With Extremely Low Damping" *IEEE Magnetics Letters* **5** (2014).
5. Murong Lang et al, "Proximity Induced High-Temperature Mangetic Order in Topological Insulator - Ferrimagnetic Insulator Heterostructure," *Nano Letters* **14**, 3459-3465 (2014).